Multimodality Imaging of Neurodegenerative Processes: Part 1, The Basics and Common Dementias

Erica L. Martin-Macintosh[1]
Stephen M. Broski[1]
Geoffrey B. Johnson[1]
Christopher H. Hunt[1,2]
Ethany L. Cullen[1]
Patrick J. Peller[1,3]

OBJECTIVE. Multimodality imaging plays an important role in the structural and functional characterization of neurodegenerative conditions. This article illustrates the basic concepts of anatomic, metabolic, and amyloid imaging and describes the application of a multimodality approach in the evaluation of patients with the more common neurodegenerative dementia processes. Proper utilization of clinically available imaging techniques allows greater insight into these common disease processes.

CONCLUSION. Recognizing the strength of combined anatomic, metabolic, and amyloid imaging can allow a more complete and confident assessment of patients with common degenerative dementias. This added knowledge can improve clinical care, allow initiation of appropriate therapies and counseling, and improve prognostication.

Dementia refers to a loss of cognitive function that disrupts the activities of daily living. It affects 7–8% of individuals older than 65 years old and 30% of individuals older than 80 years old [1]. Alzheimer disease (AD) is the most common dementia, accounting for 50–80% of cases, whereas dementia with Lewy bodies (DLB) and frontotemporal dementia (FTD) are less common subtypes [2]. The diagnosis requires exclusion of short-term cognitive dysfunction (delirium), psychiatric conditions, and treatable nonneurodegenerative intracranial conditions. Accurate diagnosis of the dementia subtype is particularly important because therapy and prognosis vary significantly with each entity.

Historically, dementia imaging focused on ruling out treatable nonneurodegenerative causes, such as mass lesions, infarcts, subdural hematomas, or normal-pressure hydrocephalus. However, in the past decade, dementia imaging has transitioned to a role of ruling in early neurodegenerative processes. Hence, the American Academy of Neurology [3] and ACR Appropriateness Criteria [4] recommend anatomic neuroimaging for patients with clinical findings concerning for dementia and suggest ^{18}F-FDG PET/CT for problem-solving purposes to identify specific patterns of neurodegenerative disease [3, 4].

In patients with dementia, anatomic imaging with conventional MRI is frequently unrevealing because structural findings, such as atrophy, typically lag behind clinical symptoms. However, modern MRI techniques reveal structural abnormalities and signal intensity alterations at increasingly earlier stages of disease. Metabolic imaging with FDG PET/CT allows identification of cellular dysfunction and death often before anatomic changes are visible on MRI. Quantitative analyses of both metabolic and anatomic data are critical because these analyses allow earlier and more accurate diagnoses of cellular dysfunction and atrophy, respectively. Quantitative analyses may also identify patterns of change specific to different neurodegenerative processes. Molecular imaging with amyloid-binding PET can identify patients at risk for developing dementia, mark very early stages of the disease process, and help differentiate dementia due to amyloid-related processes from other nonamyloid neurodegenerative processes.

The purpose of this article is to build on readers' knowledge of the classic anatomic appearances of common neurodegenerative processes by highlighting complementary metabolic and amyloid imaging techniques (Table 1) and discussing basic clinical correlation. A multimodality approach in the evaluation of neurocognitive conditions promises earlier characterization and a better ability to prognosticate, tailor treatment, and appropriately select patients for clinical trials, counseling, and disease-modifying therapies.

Keywords: amyloid imaging, brain FDG PET/CT, dementia, neurodegenerative

DOI:10.2214/AJR.14.12842

Received March 10, 2014; accepted after revision February 10, 2016.

Based on a presentation at the ARRS 2013 Annual Meeting, Washington, DC.

[1]Department of Radiology, Division of Nuclear Radiology, Mayo Clinic, 200 First St SW, Rochester, MN 55905. Address correspondence to E. L. Martin-Macintosh (martinmacintosh.erica@gmail.com).

[2]Department of Radiology, Division of Neuroradiology, Mayo Clinic, Rochester, MN.

[3]Eka Medical Center Jakarta, Bumi Serpong Damai City, Tangerang, Indonesia.

AJR 2016; 207:871–882

0361–803X/16/2074–871

TABLE 1: Typical Imaging Patterns of Common Neurodegenerative Dementias

Entity	MRI	^{18}F-FDG PET	Amyloid PET
Alzheimer disease	Initially normal with progression of hippocampal, amygdala, and temporoparietal volume loss in advanced disease	Posterior cingulate, parietal, and medial temporal hypometabolism with extension into frontal lobes in advanced disease Symmetric or asymmetric Spares motor and visual cortex	Positive (preceding symptoms)
Vascular dementia	Leukoaraiosis Lacunar infarcts Encephalomalacia Subcortical microhemorrhages or superficial lobar macrohemorrhages suggest CAA	Focal hypometabolism corresponding to disease on MRI	Negative May be positive in CAA
Dementia with Lewy bodies	Initially normal with progression to diffuse atrophy in advanced disease	Generalized FDG hypometabolism with involvement of visual cortex "Cingulate island" sign Spares motor cortex	Positive in two-thirds of patients and normal in one-third of patients
Behavioral FTD	Initially normal with progression of frontal and anterior temporal volume loss later in disease process	Frontal and anterior temporal lobe hypometabolism with involvement of basal ganglia later in disease process	Negative
Semantic (PPA-S)	Initially normal with anterior temporal lobe and hippocampal atrophy later in disease Asymmetric, most commonly left sided	Left anterior temporal lobe hypometabolism, especially superior, middle, and inferior temporal gyri, and uncus Less commonly this may affect right hemisphere, but is an asymmetric process	Typically negative
Agrammatic or nonfluent (PPA-G)	Initially normal with perisylvian cortex, inferior frontal gyrus, and superior temporal gyrus atrophy later in disease Asymmetric, most commonly left sided	Left middle and inferior frontal lobe (Broca's area) and precentral gyri hypometabolism Less commonly this may affect right hemisphere, but is an asymmetric process	Typically negative
Logopenic (PPA-L)	Initially normal with posterior perisylvian and parietal atrophy later in disease Asymmetric, most commonly left sided	Left posterior temporal and parietal hypometabolism, especially middle and inferior frontal and superior temporal gyri Less commonly this may affect right hemisphere, but is an asymmetric process	Negative or positive suggesting the potential for 2 subtypes (Alzheimer disease– and FTD-related)

Note—CAA = cerebral amyloid angiopathy, FTD = frontotemporal dementia, PPA = primary progressive aphasia.

Imaging Techniques

Anatomic Imaging

MRI and, to a lesser degree, CT can be useful in excluding nonneurodegenerative causes of dementia and are often ordered before molecular imaging. Both modalities have been approved by the U.S. Food and Drug Administration (FDA) and Centers for Medicare & Medicaid Services (CMS) for the evaluation of dementia and can show characteristic patterns of volume loss in late-stage neurodegenerative processes. However, MRI is preferable to CT because of its greater sensitivity [1]. Classic MRI sequences for dementia evaluation include sagittal and axial T1-weighted, axial T2-weighted, axial T2-weighted FLAIR (Fig. 1A), axial DWI, and susceptibility T2*-weighted gradient-echo sequences and 3D volume acquisitions. Additional sequences including coronal FLAIR and gadolinium-enhanced sequences may be considered on an individual basis. This imaging protocol targets evaluation for surgically treatable lesions, the extent of vascular disease, and patterns of cortical atrophy with an emphasis on the hippocampi, precuneus, temporal and frontal lobes, midbrain, and pons [5]. Quantitative analysis including manual and semiautomated volumetry has been used specifically in the setting of entorhinal and hippocampal atrophy in AD. Advanced techniques including diffusion-tensor imaging, functional imaging, spectroscopy, and arterial spin labeling may also provide valuable complementary information. Based on the recommendations from the American Academy of Neurology [3] and ACR Appropriateness Criteria [4], these techniques are currently recommended as research tools [6] and should be used alongside additional neurodegenerative process biomarkers discussed later in this article.

Metabolic Imaging

FDG PET/CT detects neurodegenerative processes earlier than anatomic imaging and relies on recognition of the classic patterns of hypometabolism to identify and differentiate among these processes. The brain is an obligate glucose user, and therefore neuronal activity is directly correlated to glucose metabolism. FDG, a glucose analog, can be used to measure regional glucose consumption in the brain because it becomes trapped in cells

after irreversible phosphorylation. Thus, regions of neuronal dysfunction correspond to decreased glucose metabolism [7, 8]. However, evaluating levels of glucose metabolism in the brain can be subjective, similar to assessing parenchymal atrophy on MRI (Fig. 1B). This makes quantitation vital in the interpretation of brain FDG PET/CT. Quantification software increases both the sensitivity and specificity of the examination. The software currently used at our institution samples the FDG PET dataset at thousands of cortical locations to create a 3D stereotactic surface projection (SSP) (Fig. 1C). An age-matched Z-score can be generated for each cortical region by comparing with a normative database on a voxel-by-voxel basis. These Z-score data can then be displayed on 3D SSP brain surface maps (Fig. 1D) for visual inspection [9]. However, there are multiple acceptable quantitative programs both with and without SSP displays.

To date, the FDA has approved FDG PET/CT only for the differentiation of AD from FTD. Even though neurodegenerative processes other than AD and FTD can be diagnosed with the help of FDG PET/CT, as described later in this article, the use of FDG PET/CT for these purposes is currently considered off-label.

Amyloid Imaging

There has been a strong push for the development of molecular imaging agents to aid in the early and accurate diagnosis of neurodegenerative processes. The presence of β-amyloid plaque deposits in the cerebral cortex seen at autopsy in patients with AD prompted the development of experimental radiotracers, such as Pittsburg Compound B (PIB). Carbon 11–labeled PIB has a short half-life of approximately 20 minutes that requires production from an onsite cyclotron and rapid imaging. Because of this short half-life, longer-lived radioisotopes that can be shipped were developed. For example, ^{18}F-florbetapir, ^{18}F-flutemetamol, and ^{18}F-florbetaben are three agents now approved by the FDA for identification of β-amyloid deposition in the cerebral cortex [10–12]. With the successful development of amyloid imaging agents, it is now clear that amyloid deposition occurs long before the clinical appearance of mild cognitive impairment (MCI) or dementia, perhaps by 15 or more years [13, 14]. However, CMS has not approved these imaging agents for clinical use to date, and therefore they are not widely reimbursed. The current appropriate use criteria from the Amyloid Imaging Task Force [15], a joint effort of the Alzheimer's Association and the Society of Nuclear Medicine and Molecular Imaging, state that amyloid PET should be considered only if there is significant diagnostic uncertainty after comprehensive evaluation and if the results are anticipated to increase diagnostic certainty and to alter management [16].

Amyloid imaging is currently interpreted in a binary fashion as either positive or negative for the presence of β-amyloid in the brain. It is unclear whether additional diagnostic information will be gleaned from identifying specific patterns of amyloid deposition. Currently approved amyloid imaging agents bind nonspecifically to normal white matter but show low background activity in normal gray matter. Therefore, in healthy patients, greater uptake is seen in the white matter than in the gray matter, resulting in a well-delineated gray matter–white matter interface (Fig. 1E). In abnormal patients, amyloid is deposited in cortical gray matter so that there is a subjective loss of this normal gray matter–white matter delineation. Fortunately, amyloid imaging findings in patients with MCI or AD due to amyloid are not subtle. Because the cerebellar gray matter rarely accumulates amyloid, it can be used as an internal control.

A quantitative analysis can be performed using the ratio of the standardized uptake values (SUVs) of the cerebral cortex to the cerebellar cortex. For example, when using florbetapir, an SUV ratio of cerebral cortex to cerebellar cortex of more than 1.1–1.2 is considered positive for amyloid deposition [17]. However, normal SUV ratio ranges appear to vary significantly from one amyloid agent to another [18–20]. As opposed to FDG PET/CT of the brain, for which quantitative assessment is essential, there has been better correlation of visual assessment than quantitative assessment in the interpretation of amyloid PET [21, 22]. Interestingly, regions of amyloid deposition may be different than areas of focal atrophy or hypometabolism revealed on MRI and FDG PET/CT [23, 24].

The results of amyloid PET have significant clinical implications. Patients with positive amyloid studies have a higher risk of conversion to dementia than patients with negative studies. Furthermore, a negative amyloid PET study nearly negates the potential of underlying AD, with a negative predictive value of 100% in some studies [25].

Common Neurodegenerative Processes

Alzheimer Disease

AD represents the underlying cause of approximately 50–80% of all cases of dementia. The incidence of AD doubles every 5 years after the age of 60 years old [26]. Clinically, this disease progresses with decline in episodic memory with or without language or visual difficulties. The prodromal stage of MCI has been defined as cognitive decline greater than expected for age but not interfering with activities of daily living [27]. Progression to AD has been reported in approximately 10–15% of patients with MCI annually [14, 28].

Anatomic imaging—It is difficult to differentiate MCI and AD from cortical atrophy related to normal aging using MRI [27] (Fig. 2A). Typical structural changes seen in AD occur late in the disease process and include disproportionate hippocampal, amygdala, and temporoparietal volume loss with sparing of the primary sensorimotor cortex (Fig. 3A). Volumetric software for quantifying hippocampal volumes can be helpful. Visible change within a 12- to 18-month time period on serial imaging has been reported to increase the sensitivity for the diagnosis of AD [29]. Additional studies indicate that visual rating of medial temporal lobe atrophy on MRI in the coronal plane shows fair-to-good intraobserver reliability [30]. Typically this atrophy is bilateral and symmetric and occurs at a more rapid rate than atrophy occurring from normal aging. To complicate MRI interpretation, atypical findings of AD may include little or no hippocampal atrophy and focal asymmetric cortical atrophy. Specifically, precuneus atrophy may be seen in early-onset AD in the relative absence of hippocampal atrophy [31].

Metabolic imaging—At the earliest stages, hypometabolism may be limited to the posterior cingulate cortex and precuneus. With disease progression, characteristic temporoparietal hypometabolism develops even before structural changes (Figs. 3B–3D). With advanced AD, there is broadly distributed cortical hypometabolism that frequently extends into the frontal lobes. The typical AD pattern of hypometabolism spares the sensory, motor, visual, and cerebellar cortexes; basal ganglia; and thalami [7, 32]. Most frequently, this pattern is bilateral; however, asymmetry is common and can be severe [33]. FDG PET/CT has excellent performance in the diagnosis of AD; large-scale studies have reported a sensitivity of 93–97% and specificity of 86% of

PET for the diagnosis of AD [34]. Patients with MCI can show a spectrum of findings, with hypometabolism ranging from a pattern seen in well-established AD to only mild abnormality (Figs. 2B–2D). FDG PET/CT can provide important prognostic information in this patient population because more severe baseline hypometabolism and progressive hypometabolism in MCI patients are associated with a higher rate of progression to AD and associated functional decline [33, 35].

Amyloid imaging—Amyloid PET is positive in patients with AD and may show cortical uptake in the frontal, cingulate, precuneus, parietal, and lateral temporal cortexes [36] (Figs. 2E and 3E). Correlation with the pattern of hypometabolism seen on FDG PET/CT is helpful in differentiating AD from DLB because DLB is often amyloid-positive [37, 38]. Rarely, severe atrophy can mislead the interpreter into assuming that there is low gray matter activity, resulting in a false-negative interpretation [25]. Care should be taken to evaluate anatomic imaging alongside the amyloid PET data.

Vascular Dementia

Underlying vascular disease is reported as a contributing factor in up to 45% of all patients with dementia [39]. Clinically, vascular dementia may present with sudden onset of dysfunction or stepwise deterioration in patients with risk factors for stroke, systemic vascular disease, or a history of stroke. Because white matter disease increases with age, there remains uncertainty about the severity of disease needed to diagnose vascular dementia. Some sources suggest that approximately 25% of white matter needs to be affected; however, this imaging pattern alone does not imply clinical findings of dementia. Vascular dementia is most commonly sporadic because of underlying pathologic conditions such as atherosclerosis or cerebral amyloid angiopathy (CAA). More rarely, vascular dementia may be heritable, such as in cerebral autosomal-dominant arteriopathy with subcortical infarcts and leukoencephalopathy (CADASIL) [1, 39]. Complicating matters is the fact that the coexistence of vascular dementia and AD is common given the shared risk factors in an aging population [1, 40].

Anatomic imaging—Large-vessel disease may result in a typical cerebral vascular distribution of cortical or subcortical infarcts. However, small-vessel disease is more common, resulting in focal or confluent regions of subcortical and periventricular increased signal intensity on T2-weighted FLAIR imaging, sparing of the subcortical U fibers, and small lacunar infarcts [23] (Fig. 4A). Posteriorly distributed white matter disease with macro- or microhemorrhages manifested as areas of signal loss on T2*-weighted imaging can be seen in CAA. Neuroimaging criteria have been devised for assessing cerebrovascular disease and dementia, but to date these criteria are nonspecific in distinguishing between poststroke patients and dementia patients [41]. However, in the setting of clinical dementia, the anatomic distribution of vascular disease often correlates with patient symptoms [2].

Molecular imaging—FDG PET/CT is infrequently ordered in the evaluation of patients with clinical findings suggestive of vascular dementia. However, FDG PET/CT can be helpful when an additional diagnosis of AD is being considered [42]. FDG PET/CT hypometabolism tends to be focal and severe, correlating with regions of white matter disease and postinfarct encephalomalacia on MRI [43, 44] (Figs. 4B–4D). Correlating decreased FDG uptake with areas of signal abnormality on MRI is critical in patients with vascular dementia because interpretation of metabolic imaging alone could easily lead to a misdiagnosis.

Amyloid imaging—Amyloid PET is typically negative in patients with pure vascular dementia. However, amyloid deposition can be seen in patients with CAA, and some studies indicate that the sites of amyloid deposition correspond to future locations of hemorrhage [45]. Future research may prove integral in identifying patients at risk for CAA-related hemorrhage and patients who may benefit from anti–amyloid deposition immunotherapies [46].

Frontotemporal Dementia

Estimated to contribute to less than 10% of all dementia cases, FTD is the third most common type of dementia and the most common type of dementia in patients younger than 60 years old [44]. Clinical symptoms include behavioral issues, affective symptoms, and language disorders. FTD subtypes include behavioral FTD and language-predominant cognitive decline FTD, the latter of which is referred to as primary progressive aphasia (PPA). PPA is further classified into semantic, agrammatic or nonfluent, and logopenic PPA variants [47, 48]. Compared with AD, FTD usually has an earlier onset and more rapid progression. FTD likely represents several different types of neurodegenerative processes, and the patterns of imaging findings can be strikingly different. Early differentiation of FTD from AD is clinically important because symptoms caused by FTD do not respond to traditional therapies approved for AD, such as donepezil; in fact, donepezil may even decrease the quality of life in patients with FTD. Partly because of this therapeutic difference, FDG PET/CT has been approved by the FDA and CMS for the evaluation of dementia if the differential diagnostic consideration is AD versus FTD.

Anatomic imaging—The structural findings in patients with behavioral FTD include symmetric or asymmetric frontal or temporal lobe atrophy with relative sparing of the parietal and occipital lobes [49]. Atrophy can be severe with so-called "knife blade gyri," but this is a late finding in the behavioral FTD process (Fig. 5A). The following characteristic patterns of atrophy have been described for the language-predominant cognitive decline FTD (PPA) subtypes: left anterior temporal lobe and hippocampal atrophy in semantic PPA; left perisylvian cortex, inferior frontal gyrus (Broca area), and superior temporal gyrus atrophy in agrammatic or nonfluent PPA; and left posterior perisylvian or parietal atrophy in logopenic PPA [50].

Metabolic imaging—FDG PET/CT shows distinct patterns of hypometabolism in the frontal and anterior temporal lobes in behavioral FTD with later involvement of the parietal lobes [51] (Figs. 5B–5D). Semantic PPA has a pattern of asymmetric (left greater than right) anterior temporal hypometabolism [47] with extension into the frontoparietal cortex later in the disease process [52]. Agrammatic or nonfluent PPA typically shows hypometabolism specifically involving the middle and inferior aspect of the left frontal lobe and precentral gyrus. With logopenic PPA, PET commonly reveals left lateral temporoparietal lobe and left middle parietal lobe hypometabolism [53, 54].

Amyloid imaging—Amyloid PET findings are negative in patients with behavioral FTD, which is particularly helpful in differentiating these patients from those with early-onset AD [55]. This difference is especially helpful in the diagnosis of language-predominant cognitive decline FTD given the significant overlap in clinical findings with AD.

Dementia With Lewy Bodies

DLB is increasingly recognized as a cause of dementia in patients older than 60 years old and now possibly represents 1 in every 25 de-

mentia cases in the community and 1 in every 12 cases in secondary care centers [56, 57]. Symptoms include dementia with visual hallucinations, parkinsonism, and REM sleep behavior disorder. In this entity, dementia symptoms occur before parkinsonism in contrast to Parkinson disease with dementia in which dementia occurs in the setting of well-established parkinsonism [58, 59]. Approximately 70–90% of patients with DLB show parkinsonian symptoms at the time of cognitive symptoms [59]. Early differentiation of DLB from AD is critical because DLB symptoms may respond to neuroleptic therapy, thus improving the quality of life of patients with DLB.

Anatomic imaging—The imaging findings of DLB are nonspecific, with varying patterns of cortical and white matter volume loss and relative preservation of the hippocampi [60]. Despite visual symptoms reported in patients with DLB, occipital lobe atrophy is not typically observed [61] (Fig. 6A).

Metabolic imaging—Characteristic FDG PET/CT findings of DLB can overlap with those of AD and include hypometabolism in the visual cortex, both occipital lobes, and both parietooccipital regions (Figs. 6B–6D). In contrast to DLB, AD typically spares the visual cortex [62], and this difference is an important discriminating feature. Patients with DLB may also show sparing of the posterior cingulate relative to the precuneus and cuneus, creating the so-called "cingulate island" sign, which may also assist in differentiation of DLB from AD [63].

Amyloid imaging—Amyloid PET is positive in approximately two-thirds of patients with DLB and therefore does not help in the differentiation of DLB from AD but could be used in conjunction with anatomic imaging and FDG PET/CT [37, 38] (Fig. 6E).

Dopaminergic imaging—This topic will not be covered in detail here, but we direct readers to the literature [64, 65]. When a differential diagnosis of DLB versus AD is considered, ^{123}I-ioflupane SPECT (DaT scan) may be helpful because it will show positive findings in patients with DLB and normal findings in patients with AD [66].

Conclusion

Recognizing the strength of combined anatomic, metabolic, and amyloid imaging can allow a more complete and confident assessment of patients with common degenerative dementias. This added knowledge can improve clinical care, allow initiation of appropriate therapies and counseling, and improve prognostication.

Acknowledgments

We thank Sonia Watson and Andrea Moran for their assistance with the preparation and editing of our manuscript.

References

1. Dormont D, Seidenwurm DJ. Dementia and movement disorders. *AJNR* 2008; 29:204–206
2. Kanekar S, Poot JD. Neuroimaging of vascular dementia. *Radiol Clin North Am* 2014; 52:383–401
3. Knopman DS, DeKosky ST, Cummings JL, et al. Practice parameter: diagnosis of dementia (an evidence-based review)—report of the Quality Standards Subcommittee of the American Academy of Neurology. *Neurology* 2001; 56:1143–1153
4. Wippold FJ 2nd, Brown DC, Broderick DF, et al. ACR Appropriateness Criteria: dementia and movement disorders. https://acsearch.acr.org/docs/69360/Narrative/. Published 1996. Updated 2014. Accessed December 8, 2014
5. Harper L, Barkhof F, Scheltens P, Schott JM, Fox NC. An algorithmic approach to structural imaging in dementia. *J Neurol Neurosurg Psychiatry* 2014; 85:692–698
6. Graff-Radford J, Kantarci K. Magnetic resonance spectroscopy in Alzheimer's disease. *Neuropsychiatr Dis Treat* 2013; 9:687–696
7. Hoffman JM, Welsh-Bohmer KA, Hanson M, et al. FDG PET imaging in patients with pathologically verified dementia. *J Nucl Med* 2000; 41:1920–1928
8. Nasrallah I, Dubroff J. An overview of PET neuroimaging. *Semin Nucl Med* 2013; 43:449–461
9. Minoshima S, Frey KA, Koeppe RA, Foster NL, Kuhl DE. A diagnostic approach in Alzheimer's disease using three-dimensional stereotactic surface projections of fluorine-18-FDG PET. *J Nucl Med* 1995; 36:1238–1248
10. Landau SM, Breault C, Joshi AD, et al. Amyloid-beta imaging with Pittsburgh compound B and florbetapir: comparing radiotracers and quantification methods. *J Nucl Med* 2013; 54:70–77
11. Syed YY, Deeks E. [(18)F]Florbetaben: a review in beta-amyloid PET imaging in cognitive impairment. *CNS Drugs* 2015; 29:605–613
12. Vandenberghe R, Van Laere K, Ivanoiu A, et al. ^{18}F-flutemetamol amyloid imaging in Alzheimer disease and mild cognitive impairment: a phase 2 trial. *Ann Neurol* 2010; 68:319–329
13. Chételat G, La Joie R, Villain N, et al. Amyloid imaging in cognitively normal individuals, at-risk populations and preclinical Alzheimer's disease. *Neuroimage Clin* 2013; 2:356–365
14. Jack CR Jr, Knopman DS, Jagust WJ, et al. Hypothetical model of dynamic biomarkers of the Alzheimer's pathological cascade. *Lancet Neurol* 2010; 9:119–128
15. Johnson KA, Minoshima S, Bohnen NI, et al.; Alzheimer's Association; Society of Nuclear Medicine and Molecular Imaging; Amyloid Imaging Taskforce. Appropriate use criteria for amyloid PET: a report of the Amyloid Imaging Task Force, the Society of Nuclear Medicine and Molecular Imaging, and the Alzheimer's Association. *Alzheimers Dement* 2013; 9:e-1–e-16
16. Sánchez-Juan P, Ghosh PM, Hagen J, et al. Practical utility of amyloid and FDG-PET in an academic dementia center. *Neurology* 2014; 82:230–238
17. Fleisher AS, Chen K, Liu X, et al. Using positron emission tomography and florbetapir F18 to image cortical amyloid in patients with mild cognitive impairment or dementia due to Alzheimer disease. *Arch Neurol* 2011; 68:1404–1411
18. Jack CR Jr, Wiste HJ, Weigand SD, et al. Amyloid-first and neurodegeneration-first profiles characterize incident amyloid PET positivity. *Neurology* 2013; 81:1732–1740
19. Johnson KA, Sperling RA, Gidicsin CM, et al.; AV45-A11 Study Group. Florbetapir (F18-AV-45) PET to assess amyloid burden in Alzheimer's disease dementia, mild cognitive impairment, and normal aging. *Alzheimers Dement* 2013; 9(suppl 5):S72–S83
20. Sabri O, Seibyl J, Rowe C, Barthel H. Beta-amyloid imaging with florbetaben. *Clin Transl Imaging* 2015; 3:13–26
21. Lowe VJ, Kemp BJ, Jack CR Jr, et al. Comparison of ^{18}F-FDG and PiB PET in cognitive impairment. *J Nucl Med* 2009; 50:878–886
22. Ng S, Villemagne VL, Berlangieri S, et al. Visual assessment versus quantitative assessment of ^{11}C-PIB PET and ^{18}F-FDG PET for detection of Alzheimer's disease. *J Nucl Med* 2007; 48:547–552
23. Bhogal P, Mahoney C, Graeme-Baker S, et al. The common dementias: a pictorial review. *Eur Radiol* 2013; 23:3405–3417
24. Klunk WE, Engler H, Nordberg A, et al. Imaging brain amyloid in Alzheimer's disease with Pittsburgh compound-B. *Ann Neurol* 2004; 55:306–319
25. Nordberg A, Carter SF, Rinne J, et al. A European multicentre PET study of fibrillar amyloid in Alzheimer's disease. *Eur J Nucl Med Mol Imaging* 2013; 40:104–114
26. Qiu C, Kivipelto M, von Strauss E. Epidemiology of Alzheimer's disease: occurrence, determinants, and strategies toward intervention. *Dialogues Clin Neurosci* 2009; 11:111–128
27. Gauthier S, Reisberg B, Zaudig M, et al. Mild cognitive impairment. *Lancet* 2006; 367:1262–1270
28. Jack CR Jr. Alzheimer disease: new concepts on its neurobiology and the clinical role imaging will play. *Radiology* 2012; 263:344–361
29. Leung KK, Clarkson MJ, Bartlett JW, et al. Robust atrophy rate measurement in Alzheimer's disease using multi-site serial MRI: tissue-specific intensity normalization and parameter selection. *Neuroimage* 2010; 50:516–523
30. Scheltens P, Launer LJ, Barkhof F, Weinstein HC,

van Gool WA. Visual assessment of medial temporal lobe atrophy on magnetic resonance imaging: interobserver reliability. *J Neurol* 1995; 242:557–560

31. Vernooij MW, Smits M. Structural neuroimaging in aging and Alzheimer's disease. *Neuroimaging Clin N Am* 2012; 22:33–55, vii–viii
32. Mosconi L, Tsui WH, Herholz K, et al. Multicenter standardized ^{18}F-FDG PET diagnosis of mild cognitive impairment, Alzheimer's disease, and other dementias. *J Nucl Med* 2008; 49:390–398
33. Landau SM, Harvey D, Madison CM, et al. Associations between cognitive, functional, and FDG-PET measures of decline in AD and MCI. *Neurobiol Aging* 2011; 32:1207–1218
34. Mehta L, Thomas S. The role of PET in dementia diagnosis and treatment. *Appl Radiol* 2012; May:8–15
35. Zhang S, Han D, Tan X, Feng J, Guo Y, Ding Y. Diagnostic accuracy of 18 F-FDG and 11 C-PIB-PET for prediction of short-term conversion to Alzheimer's disease in subjects with mild cognitive impairment. *Int J Clin Pract* 2012; 66:185–198
36. Wolk DA, Price JC, Saxton JA, et al. Amyloid imaging in mild cognitive impairment subtypes. *Ann Neurol* 2009; 65:557–568 [Erratum in *Ann Neurol* 2009; 66:123]
37. Rowe CC, Villemagne VL. Brain amyloid imaging. *J Nucl Med* 2011; 52:1733–1740
38. Rowe CC, Ng S, Ackermann U, et al. Imaging beta-amyloid burden in aging and dementia. *Neurology* 2007; 68:1718–1725
39. Wardlaw JM, Smith C, Dichgans M. Mechanisms of sporadic cerebral small vessel disease: insights from neuroimaging. *Lancet Neurol* 2013; 12:483–497
40. Korczyn AD, Vakhapova V, Grinberg LT. Vascular dementia. *J Neurol Sci* 2012; 322:2–10
41. Ballard CG, Burton EJ, Barber R, et al. NINDS AIREN neuroimaging criteria do not distinguish stroke patients with and without dementia. *Neurology* 2004; 63:983–988
42. Gurol ME, Viswanathan A, Gidicsin C, et al. Cerebral amyloid angiopathy burden associated with leukoaraiosis: a positron emission tomography/magnetic resonance imaging study. *Ann Neurol* 2013; 73:529–536
43. Román G, Pascual B. Contribution of neuroimaging to the diagnosis of Alzheimer's disease and vascular dementia. *Arch Med Res* 2012; 43:671–676
44. Perry DC, Miller BL. Frontotemporal dementia. *Semin Neurol* 2013; 33:336–341
45. Ly JV, Donnan GA, Villemagne VL, et al. ^{11}C-PIB binding is increased in patients with cerebral amyloid angiopathy-related hemorrhage. *Neurology* 2010; 74:487–493
46. Gurol ME, Dierksen G, Betensky R, et al. Predicting sites of new hemorrhage with amyloid imaging in cerebral amyloid angiopathy. *Neurology* 2012; 79:320–326
47. Matías-Guiu JA, Cabrera-Martín MN, Pérez-Castejón MJ, et al. Visual and statistical analysis of ^{18}F-FDG PET in primary progressive aphasia. *Eur J Nucl Med Mol Imaging* 2015; 42:916–927
48. Wang X, Shen Y, Chen W. Progress in frontotemporal dementia research. *Am J Alzheimers Dis Other Demen* 2013; 28:15–23
49. Josephs KA. Frontotemporal lobar degeneration. *Neurol Clin* 2007; 25:683–696, vi
50. Rogalski E, Cobia D, Harrison TM, et al. Anatomy of language impairments in primary progressive aphasia. *J Neurosci* 2011; 31:3344–3350
51. Diehl-Schmid J, Grimmer T, Drzezga A, et al. Decline of cerebral glucose metabolism in frontotemporal dementia: a longitudinal ^{18}F-FDG-PET-study. *Neurobiol Aging* 2007; 28:42–50
52. Ishii K. PET approaches for diagnosis of dementia. *AJNR* 2014; 35:2030–2038
53. Madhavan A, Whitwell JL, Weigand SD, et al. FDG PET and MRI in logopenic primary progressive aphasia versus dementia of the Alzheimer's type. *PLoS One* 2013; 8:e62471
54. Josephs KA, Duffy JR, Fossett TR, et al. Fluorodeoxyglucose F18 positron emission tomography in progressive apraxia of speech and primary progressive aphasia variants. *Arch Neurol* 2010; 67:596–605
55. Vandenberghe R, Adamczuk K, Dupont P, Laere KV, Chetelat G. Amyloid PET in clinical practice: its place in the multidimensional space of Alzheimer's disease. *Neuroimage Clin* 2013; 2:497–511
56. Hansen L, Salmon D, Galasko D, et al. The Lewy body variant of Alzheimer's disease: a clinical and pathologic entity. *Neurology* 1990; 40:1–8
57. Vann Jones SA, O'Brien JT. The prevalence and incidence of dementia with Lewy bodies: a systematic review of population and clinical studies. *Psychol Med* 2014; 44:673–683
58. Lippa CF, Duda JE, Grossman M, et al. DLB and PDD boundary issues: diagnosis, treatment, molecular pathology, and biomarkers. *Neurology* 2007; 68:812–819
59. McKeith I, Mintzer J, Aarsland D, et al. Dementia with Lewy bodies. *Lancet Neurol* 2004; 3:19–28
60. Burton EJ, Karas G, Paling SM, et al. Patterns of cerebral atrophy in dementia with Lewy bodies using voxel-based morphometry. *Neuroimage* 2002; 17:618–630
61. Burton EJ, McKeith IG, Burn DJ, Williams ED, O'Brien JT. Cerebral atrophy in Parkinson's disease with and without dementia: a comparison with Alzheimer's disease, dementia with Lewy bodies and controls. *Brain* 2004; 127:791–800
62. Minoshima S, Foster NL, Sima AA, Frey KA, Albin RL, Kuhl DE. Alzheimer's disease versus dementia with Lewy bodies: cerebral metabolic distinction with autopsy confirmation. *Ann Neurol* 2001; 50:358–365
63. Graff-Radford J, Murray ME, Lowe VJ, et al. Dementia with Lewy bodies: basis of cingulate island sign. *Neurology* 2014; 83:801–809
64. Walker Z, Jaros E, Walker RW, et al. Dementia with Lewy bodies: a comparison of clinical diagnosis, FP-CIT single photon emission computed tomography imaging and autopsy. *J Neurol Neurosurg Psychiatry* 2007; 78:1176–1181
65. Broski SM, Hunt CH, Johnson GB, Morreale RF, Lowe VJ, Peller PJ. Structural and functional imaging in parkinsonian syndromes. *RadioGraphics* 2014; 34:1273–1292
66. Cummings JL, Henchcliffe C, Schaier S, Simuni T, Waxman A, Kemp P. The role of dopaminergic imaging in patients with symptoms of dopaminergic system neurodegeneration. *Brain* 2011; 134:3146–3166

(Figures start on next page)

FOR YOUR INFORMATION

The reader's attention is directed to part 2 accompanying this article, titled "Multimodality Imaging of Neurodegenerative Processes: Part 2, Atypical Dementias," which begins on page 883.

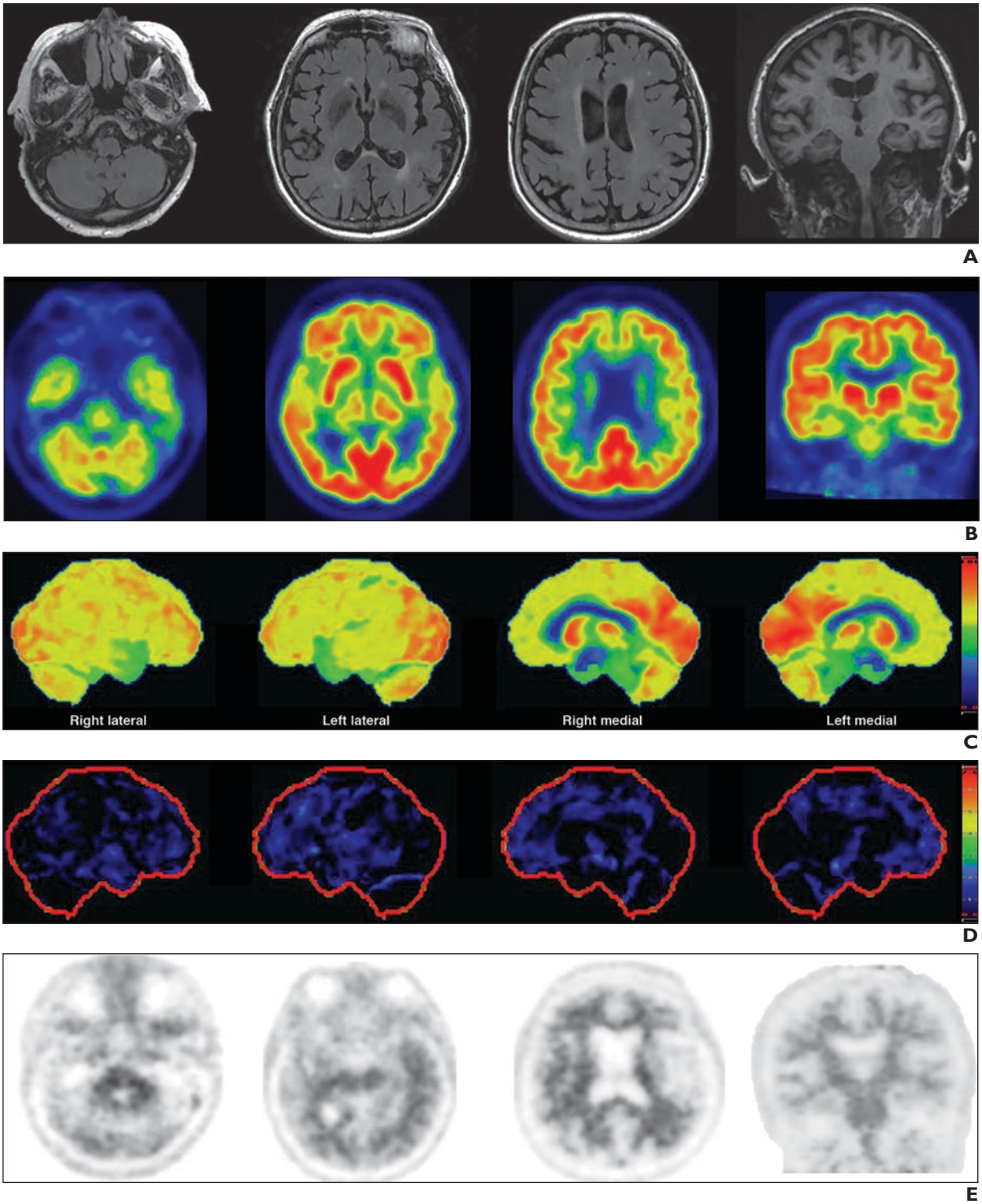

Fig. 1—83-year-old woman with normal cognition.
A, Axial T2-weighted FLAIR images at varying intracranial levels (*left image*, *middle left image*, *middle right image*) and coronal T1-weighted image at hippocampal level (*right image*) show cortical atrophy and white matter disease typical for patient's age. No anatomic abnormalities.
B, FDG PET images show normal findings including intense activity in cortical gray matter, basal ganglia, and brainstem.
C, Three-dimensional stereotactic surface projection maps (SSPs) show normal metabolism. SSPs depict normal metabolism as yellow and orange, with gradient of metabolism reduction to severe hypometabolism indicated by the colors blue and black.
D, Z-score maps show normal metabolism. Z-score maps depict normal metabolism (≤ 1 SD below mean) as blue or black, with gradient of metabolism reduction to severe hypometabolism (≥ 7 SD below mean) indicated by orange and red. Of note, color scale is opposite of that utilized on SSP maps.
E, Amyloid PET images show nonspecific white matter activity and uptake in cortical gray matter similar to cerebellar gray matter representing negative study.

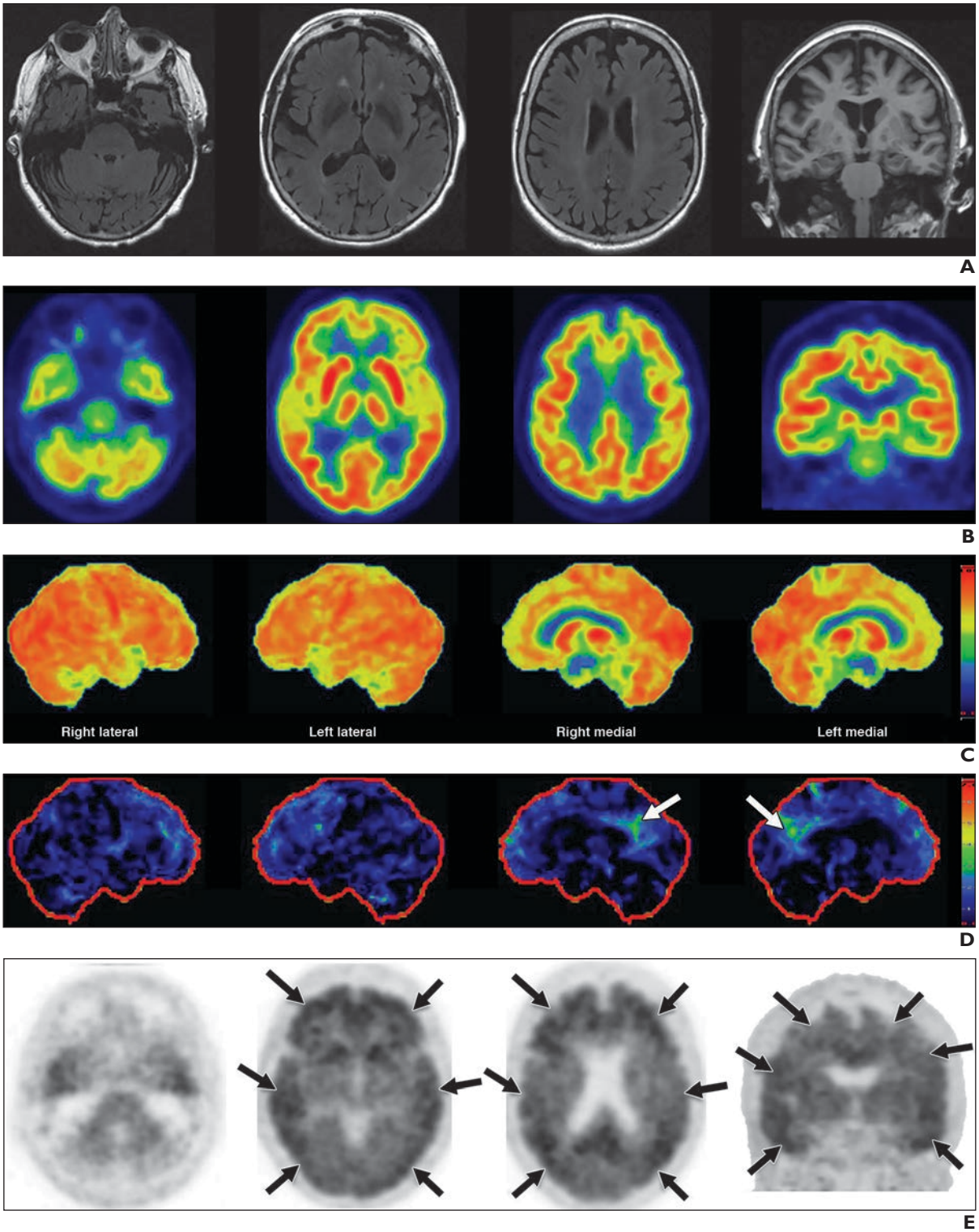

Fig. 2—79-year-old woman with mild cognitive impairment.
A, Axial T2-weighted FLAIR images at varying intracranial levels (*left image*, *middle left image*, *middle right image*), and coronal T1-weighted volumetric acquisition image (*right image*) show mild diffuse cerebral and cerebellar atrophy and normal hippocampi for age.
B–D, FDG PET images (**B**), 3D stereotactic surface projection maps (**C**), and Z-score maps (**D**) show mild temporoparietal lobe hypometabolism, right worse than left, and mildly diminished activity in posterior cingulate gyrus (*arrows*, **D**); these findings are suggestive of early Alzheimer disease.
E, Amyloid PET images reveal abnormal diffuse activity in gray matter (*arrows*) similar to white matter.

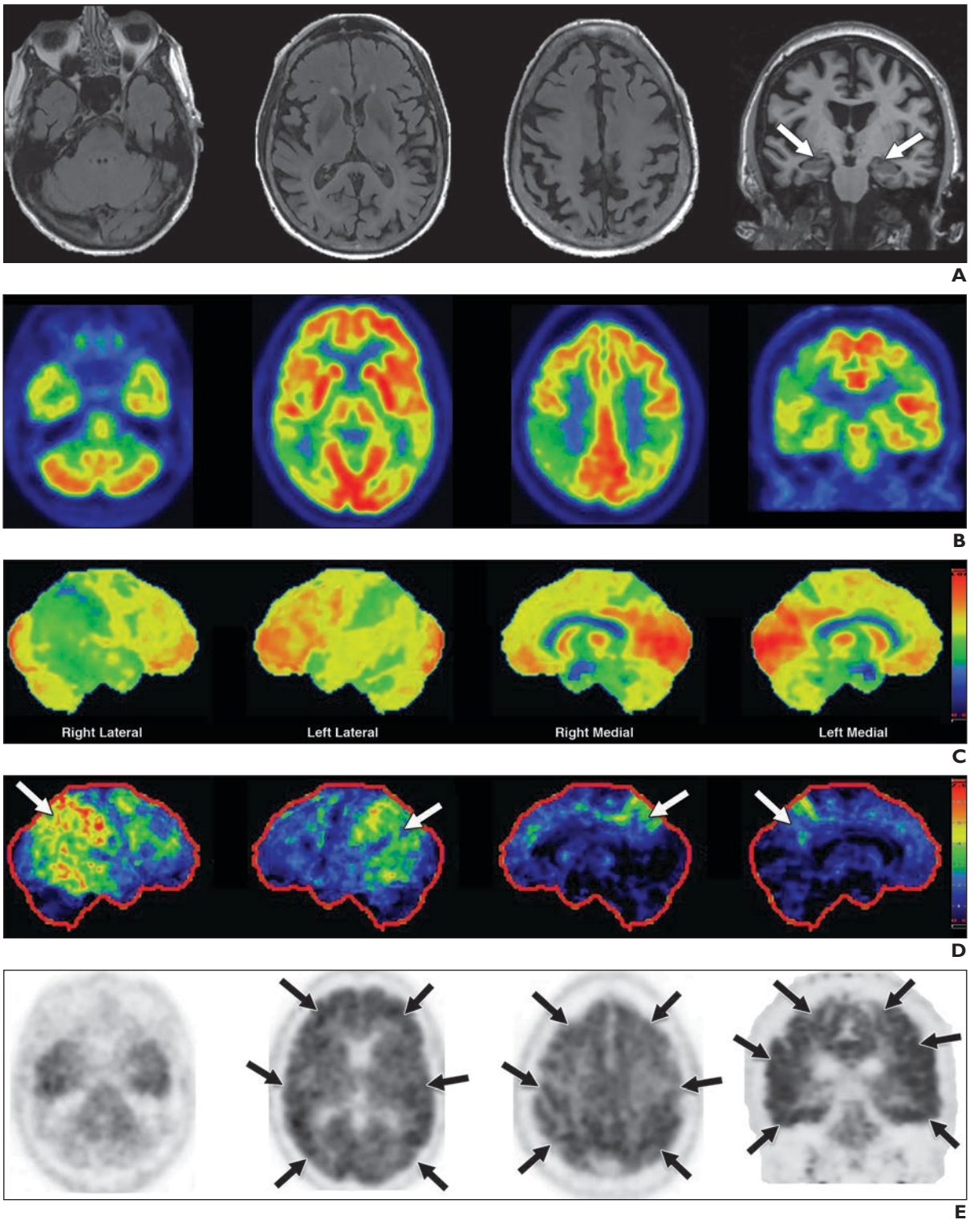

Fig. 3—56-year-old woman with Alzheimer disease.
A, Axial T2-weighted FLAIR images at varying intracranial levels (*left image*, *middle left image*, *middle right image*) and coronal T1-weighted image at hippocampal level (*right image*) show generalized cerebral volume loss that is most notable in perisylvian regions and commensurate volume loss of both hippocampal formations (*arrows*).
B, FDG PET images show marked right and moderate left temporoparietal hypometabolism. Prominent right frontal lobe hypometabolism is also noted. There is motor and visual cortex sparing.
C and **D,** Three-dimensional stereotactic surface projection maps (**C**) and Z-score maps (**D**) show significant temporoparietal lobe hypometabolism, right greater than left (> 6 SD) and bilateral posterior cingulate gyri hypometabolism (*arrows*, **D**).
E, Amyloid PET images reveal intense activity in gray matter (*arrows*) similar to activity in white matter indicating positive study.

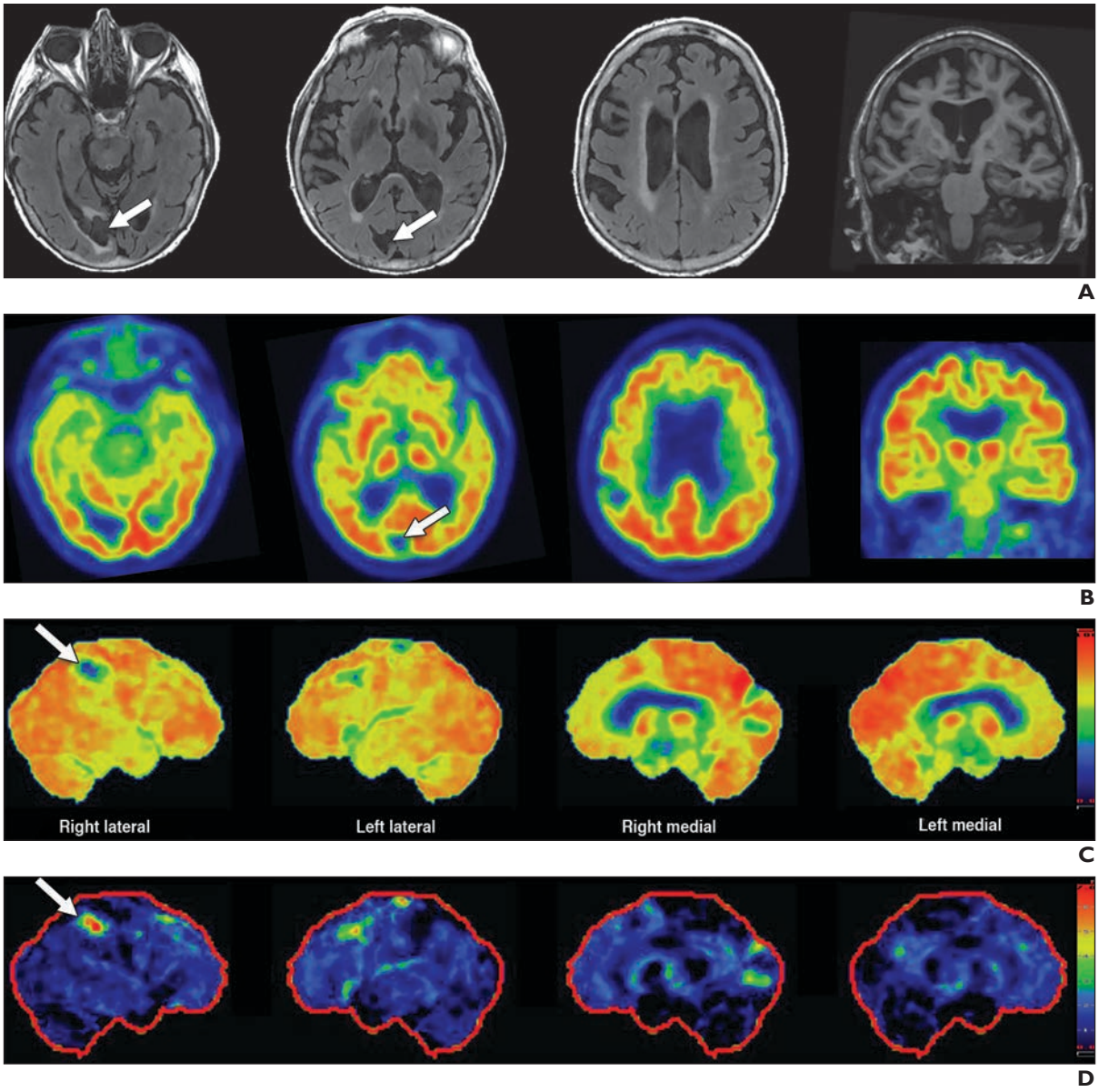

Fig. 4—84-year-old woman with multiinfarct dementia.
A, Axial T2-weighted FLAIR images at varying intracranial levels (*left image*, *middle left image*, *middle right image*), and coronal T1-weighted image at hippocampal level (*right image*) show moderate periventricular leukoaraiosis and generalized cerebral atrophy, most marked in both temporal lobes and insula. Right parafalcine occipital lobe encephalomalacia (*arrows*) is also present.
B, FDG PET images reveal focal hypometabolism in area of old right posterior cerebral artery (PCA) infarct-encephalomalacia on MRI (*arrow*).
C and **D,** Three-dimensional stereotactic surface projection maps (**C**) and Z-score maps (**D**) not only confirm hypometabolism in right PCA territory but also show multiple discrete foci of hypometabolism throughout cortex in areas of focal gyral atrophy (*arrows*). This case illustrates potential pitfall of using FDG PET/CT without anatomic imaging correlation.

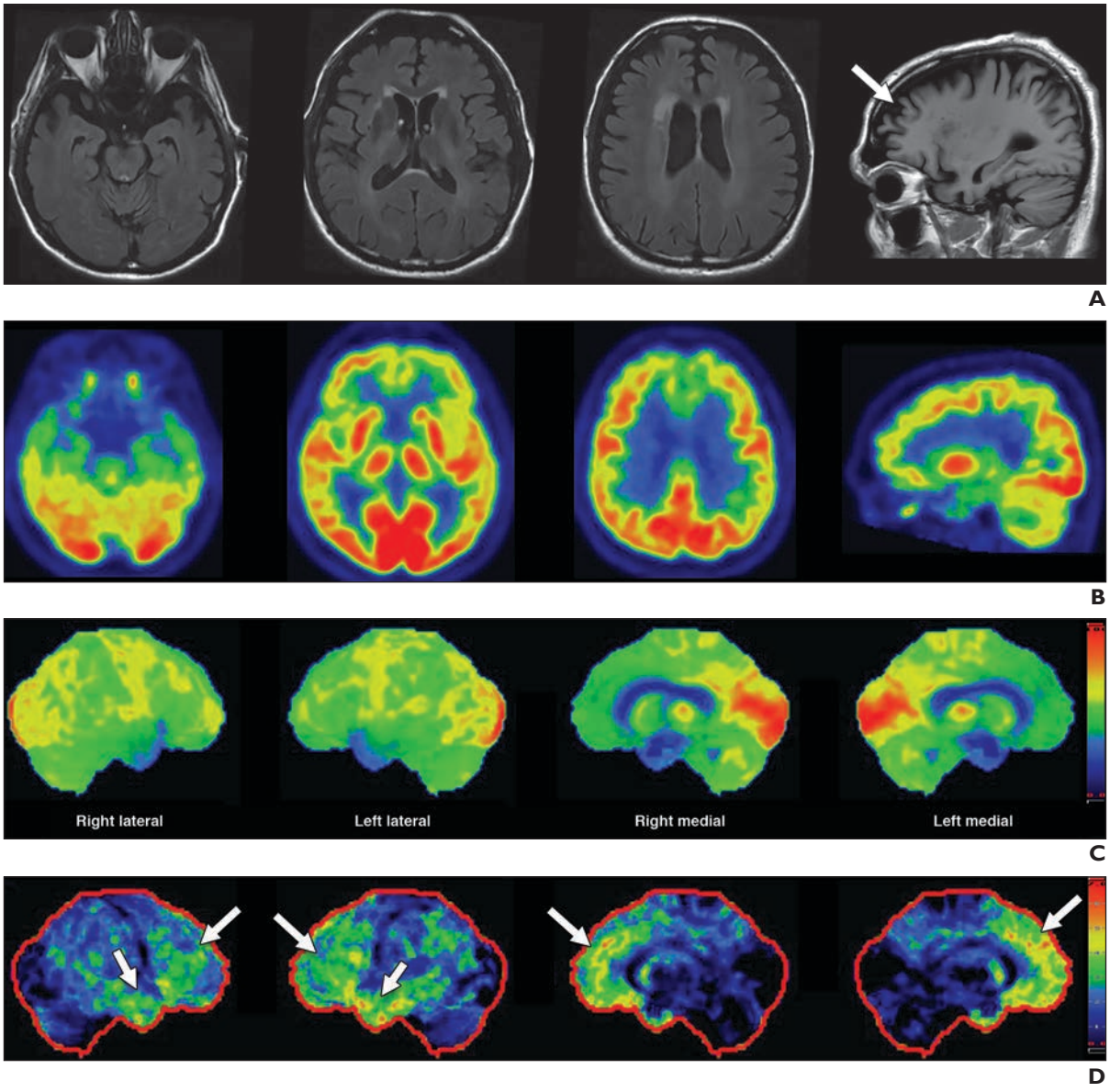

Fig. 5—59-year-old man with behavioral frontotemporal dementia.
A, Axial T2-weighted FLAIR images at varying intracranial levels (*left image*, *middle left image*, *middle right image*), and sagittal T1-weighted (*right image*) show moderate diffuse parenchymal volume loss for age and superimposed focal atrophy of the frontal and anterior temporal lobes (*arrow*).
B, FDG PET images show moderate to markedly decreased activity in both frontotemporal lobes and mildly decreased parietal lobe metabolism. Mildly decreased basal ganglia activity. There is motor cortex preservation.
C and **D,** Three-dimensional stereotactic surface projection maps (**C**) and Z-score maps (**D**) depict large areas of bilateral frontotemporal hypometabolism (3–4 SD) (*arrows*, **D**).

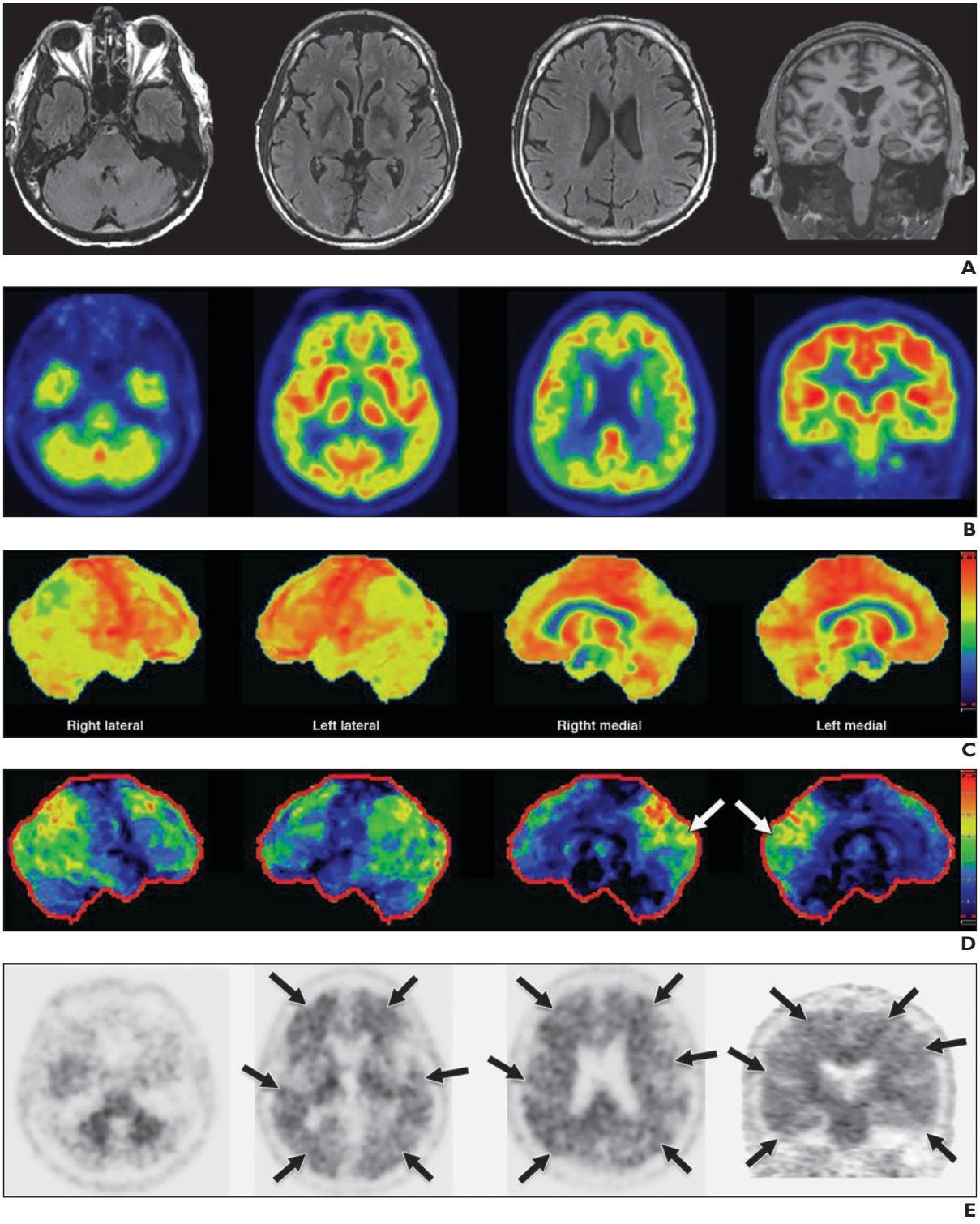

Fig. 6—63-year-old man with dementia with Lewy bodies (DLB).
A, Axial T2-weighted FLAIR images at varying intracranial levels (*left image*, *middle left image*, *middle right image*) and coronal T1-weighted image at hippocampal level (*right image*) show mild diffuse cerebral atrophy including the hippocampi.
B, FDG PET images show parietal, occipital, posterior temporal, and frontal lobe hypometabolism with motor strip preservation.
C and **D,** Three-dimensional stereotactic surface projection maps (**C**) and Z-score maps (**D**) show significant parietooccipital hypometabolism including visual cortex (3–4 SD) (*arrows*, **D**).
E, Amyloid PET images reveal abnormal diffuse activity in gray matter similar to white matter indicating positive study (*arrows*).